SEEDED VISA: A 1064nm LASER-SEEDED FEL AMPLIFIER AT THE BNL ATF

M. Dunning, G. Andonian, E. Hemsing, S. Reiche, J. Rosenzweig
UCLA Department of Physics and Astronomy, Los Angeles, CA 90095

M. Babzien, V. Yakimenko
Brookhaven National Lab, Upton, NY 11973

Abstract

An experimental study of a seeded Free Electron Laser (FEL) using the VISA undulator and a Nd:YAG seed laser will be performed at the Accelerator Test Facility (ATF) at Brookhaven National Laboratory. The study is motivated by the demand for a short Rayleigh length FEL amplifier at 1 micron to allow for high power transmission with minimal damage of transport optics. Planned measurements include transverse and longitudinal coherence, angular distribution, and wavelength spectrum of the FEL radiation. The effects of detuning the electron beam energy will be studied, with an emphasis on control of the radiation emission angles and increase of the amplifier efficiency. Results of start-to-end simulations are also presented.

INTRODUCTION

There is now a great interest in seeded FEL amplifiers, mainly due to the increased stability and preferable temporal characteristics over self-amplified spontaneous emission (SASE) sources. The output properties are a reflection of the seed laser; the energy, bandwidth, and duration of the output can be extremely stable, shot-to-shot. Additionally, in contrast to SASE, the radiation can be fully spatially and temporally coherent. One drawback is that if a short wavelength is desired (sub ∼400 nm), one must use novel schemes to seed the amplifier, such as high-gain harmonic generation (HGHG) [1].

For high single-pass gain in a relatively short undulator, it is essential to use a low emittance, high peak current electron beam.

VISA

The VISA project, housed at the BNL ATF, was initially developed as an experimental study of a high-gain SASE FEL. It consists of a 1.6 cell, S-band BNL/SLAC/UCLA photocathode gun, two SLAC type linac sections, and a four meter long, strong-focusing undulator. The beamline features a dispersive section, or dogleg, (two consecutive 20 degree dipole magnets with opposite deflection angles, separated by dispersion-matching optics) which translates the beam axis transversely. A schematic of the beamline is shown in Fig. 1, and is detailed in Ref. [2].

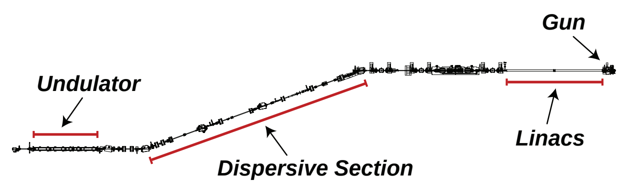

Figure 1: A schematic of the VISA beamline.

VISA I The first stage of experimentation, *VISA I*, demonstrated SASE FEL saturation at 840nm in 2001 [2]. The high peak current necessary for saturation within the four meter long undulator was achieved by exploiting the nonlinear electron bunch compression in the dogleg, as described below. Other significant experiments include the measurement of nonlinear harmonic generation [8] and microbunching [9]. The VISA I project also marked the implementation of a start-to-end simulation suite consisting of:

- `parmela` [3], for beam dynamics in the gun and linacs,
- `elegant` [4], for electron beam transport, and
- `genesis 1.3` [5], for FEL simulations.

The code suite was successfully benchmarked during the initial VISA experiments, and is still in wide use today [6, 7].

VISA Ib The next stage of experimentation, *VISA Ib*, exploited the dogleg bunch compression further, resulting in an electron beam with much higher peak current and larger energy spread. As a result, an unusually large FEL bandwidth was observed (up to 15% full width) at high gain, along with atypical far-field radiation spatial distributions [10].

Seeded VISA

The current project, *Seeded VISA*, will use a 1064nm Nd:YAG laser—the same laser used for photocathode illumination, prior to frequency quadrupling—as a coherent seed for the VISA undulator, producing fully coherent (transversely and longitudinally), narrow bandwidth FEL radiation.

Seeded VISA is also motivated by the demand for a high power, short Rayleigh length FEL for power transmission with minimal damage to transport optics. A short Rayleigh length means larger emission angles, so that the output energy is spread out spatially and does not ablate or simply melt the first optical element it contacts. To this end, the project will investigate the effect of electron beam energy detuning to control radiation emission angles, power output, and amplifier efficiency.

EXPERIMENT DESCRIPTION

Seeded VISA uses the same beamline as previous VISA experiments, with the electron beam energy lowered to achieve resonance at 1064nm. The design parameters are shown in Table 1 below.

Table 1: Seeded VISA design parameters.

Parameter	Value	Unit
Electron Beam Energy	63	MeV
Electron Beam Peak Current	55-300	A
Electron Bunch Length (RMS)	1-1.5	ps
Electron Bunch Charge	300	pC
Normalized Emittance (RMS)	2	mm-mrad
FEL Resonant Wavelength	1064	nm
Undulator parameter K	1.26	
FEL parameter ρ	0.01	
Seed Laser Energy	1	mJ
Seed Laser Pulse Length (RMS)	6	ps

Dogleg Bunch Compression

The electron beam peak current can be controlled by varying the linac phase to change the energy chirp, which along with the quadrupole settings in the dogleg, determines the compression; the shape of the current profile may also be tuned by adjusting magnets in the dogleg. The compression can be approximated by [11]

$$\Delta\sigma \approx R_{56}\delta + T_{566}\delta^2 + ..., \tag{1}$$

where σ is the bunch length, δ is the momentum error, and R_{56} and T_{566} are the first and second order transport matrix elements respectively, which depend on the dogleg geometry and beam energy. The compression is dominated by the second-order T_{566} contribution and is nonlinear. Simulation results of beam current profiles for three different stages of compression are shown in Fig. 2 below.

Time Synchronization

The seed laser/electron beam time synchronization is controlled by manually adjusting a delay line, and overlapping the SASE signal with the seed laser signal on a fast

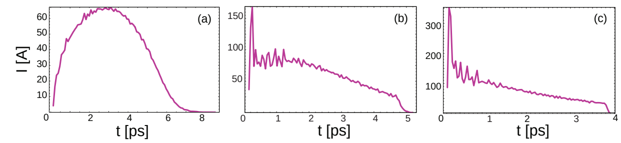

Figure 2: Current profiles at the undulator entrance for three different stages of compression, from simulation.

oscilloscope (Tektronix SCD5000, 4.5 GHz bandwidth). The SASE signal is generated by an InGaAs photodiode (Thorlabs SIR5, 5 GHz bandwidth). The laser and electron beam can thus be visually synchronized to within approximately 50 picoseconds; the final synchronization is realized by scanning the delay line in fine steps, while monitoring the FEL output energy for a sharp increase (larger than the SASE fluctuation). Seeding will be confirmed by monitoring the output spectrum, which should be narrow and consist of a single peak, in contrast to SASE, which is wider and noisier, as in Fig. 4(b,d).

The FEL radiation can be ejected and analyzed at several different ports along the undulator, or transported from the undulator exit to diagnostic stations for analysis.

PROPOSED MEASUREMENTS

Proposed measurements include the FEL pulse energy and gain curve (Coherent J3S-10 joule meter), spectrum (Ocean Optics USB2000), and far-field angular radiation distribution (CCD camera). The transverse (spatial) coherence will be measured as a function of distance along the undulator, and as a function of distance from the undulator exit, with an arrangement of slits and pepperpots [12] as in Fig. 3 below.

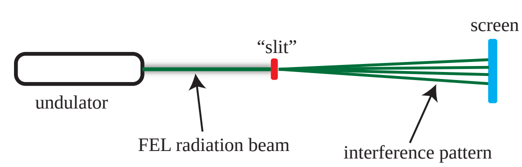

Figure 3: A schematic of the transverse coherence measurement.

Longitudinal (temporal) coherence will be measured with a FROG/Grenouille device [13], modified for a longer pulse length and finer spectral resolution. A double differential spectrometer [14] will be used to unfold the relationship between frequency and angle of the FEL radiation.

SIMULATIONS

Start-to-end simulations have been performed for various stages of compression; results are shown below in Fig. 4 for the current profile shown in Fig. 2(b).

The results for SASE with the same electron beam are shown in Fig. 4(c-d) for comparison. In the seeded sim-

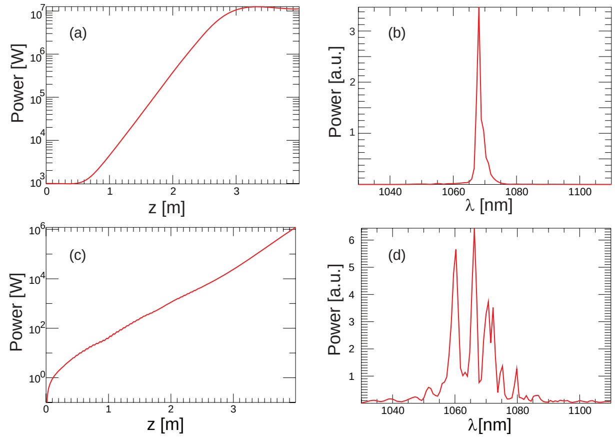

Figure 4: Gain curve and spectrum for seeding (a,b) and SASE (c,d) for comparison, for the same electron beam.

ulations, the seed laser power is 1 kW; in the SASE simulations the seed laser is absent and the FEL starts from initial shot noise. We note for the SASE case the FEL does not reach saturation and that the spectrum—and hence the temporal profile—is noisy in nature.

Electron Beam Energy Detuning Simulations were also performed for several cases of electron beam energy detuning, that is, adjusting the energy away from the resonant energy. The gain curves and far-field radiation angular distributions for two cases are shown in Fig. 5 along with the on-resonance case.

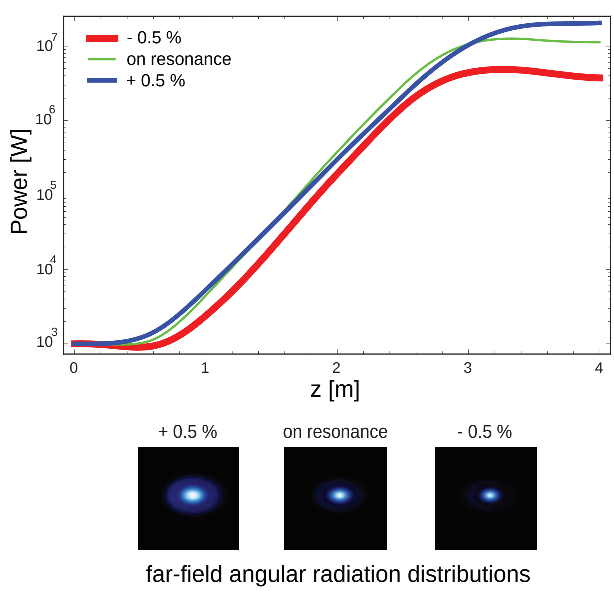

Figure 5: Gain curves (upper) for energy detuning of $+0.5\%$, on-resonance, and -0.5%, and the far-field spatial distributions (lower) for the same cases.

The results show that the gain is higher for a 0.5% increase in energy, due to the fact that the energy detuning partially offsets saturation, where the radiation field starts to give energy back to the electrons. Also, for positive detuning, the emission angles are increased and the energy per unit area, or fluence, in the far-field is decreased. Thus the radiation can transported through optical elements at higher power without damage to the elements.

EXPERIMENT STATUS

In early 2007, SASE lasing at 1064nm was achieved, with initial FEL energy measuring approximately 300 nJ/pulse. Currently, the electron beam transport is being optimized to better control beamline beta functions and dispersion, and to achieve reproducible high-gain lasing conditions. The next experiments are planned for mid-2007.

Acknowledgements

The authors graciously thank Alfredo, for many fruitful interactions.

REFERENCES

[1] A. Meseck, *Proceedings of the 2006 FEL Conference*, 226 (2006).

[2] A. Murokh, *et al.*, Phys. Rev. E **67**, 066501 (2003).

[3] L. Young and J. Billen, *Proceedings of the 2003 Particle Accelerator Conference*, 3521 (2003).

[4] M. Borland, Advanced Photon Souce LS-287 (2000).

[5] S. Reiche, Nuc. Inst. Meth. A **429**, 243 (1999).

[6] S. Reiche, *et al.*, Nuc. Inst. Meth. A **483**, 70 (2002).

[7] M. Borland, *et al.*, *Proceedings of the 2001 Particle Accelerator Conference*, 2707 (2001).

[8] A. Tremaine, *et al.*, Phys. Rev. Lett. **88**, 204801 (2002).

[9] A. Tremaine, *et al.*, Phys. Rev. E **66**, 036503 (2002).

[10] G. Andonian, *et al.*, Phys. Rev. Lett., 95, 054801 (2005).

[11] R. J. England *et al.*, Phys. Rev. STAB, **8**, 012801 (2005).

[12] R. Ischebeck, *et al.*, Nuc. Inst. Meth. A **507**, 175 (2003).

[13] R. Trebino, *Frequency Resolved Optical Gating*, Kluwer Academic Publishers, Norwell, MA (2000).

[14] G. Andonian, *et al.*, *Proceedings of the 2006 FEL Conference*, 443 (2006).

